Optimization and Application of Laser-Induced Graphene Electrodes with Nickel Hydroxide Nanoparticles for Ultrasensitive Non-Enzymatic Glucose Sensing

Rourke Sylvain, Tyler Waslawski, Verdict Vera, Grace Dykstra, Georgia Heintz, Smitha Rao*, and Yixin Liu*

Michigan Technological University, Houghton, MI, United States

*Corresponding authors: smithar@mtu.edu, yixinliu@mtu.edu

***Abstract*— This study optimizes laser-induced graphene (LIG) electrodes for electrochemical sensing by varying CO_2 laser parameters (i.e., power, speed, PPI) to convert polyimide into graphene to achieve high electrochemical performance. The electrodes are further modified with electrodeposited nickel hydroxide ($Ni(OH)_2$) nanoparticles to catalyze glucose oxidation and sense glucose in a 0.1 M NaOH solution. Through detailed morphological and electrochemical characterization, we demonstrate that multiple laser passes significantly improve the LIG electrode's electrical conductivity, surface morphology, and electrochemical performance. As a demonstration, the real-time amperometric detection of glucose using LIG-$Ni(OH)_2$ electrodes achieved an ultrahigh sensitivity of 2577 $\mu A/cm^2 \cdot mM$ glucose. Our findings provide valuable insights into the fabrication of high-performance, cost-effective, and scalable electrochemical sensors using LIG electrodes.**

Keywords—Laser-induced Graphene, LIG, Non-Enzymatic Glucose Sensor, Electrochemical Sensor, Nickle Hydroxide Electrodeposition

I. INTRODUCTION

Electrochemical sensors are crucial in a wide range of applications, including environmental monitoring, medical diagnostics, and industrial processes, offering high sensitivity, low cost, and portability [1-3]. Graphene-based electrodes, known for high conductivity and stability, are promising for electrochemical sensing, yet conventional production methods (e.g., chemical vapor deposition) remain complex and costly [4-7].

Laser-induced graphene (LIG), produced by converting polyimide into graphene using a CO_2 laser, presents a cost-effective and scalable alternative [8-10]. This method involves intricate physical and chemical transformations that are dependent on laser parameters. High-energy laser irradiation induces rapid localized heating, leading to polyimide pyrolysis [11]. This process transforms polyimide into a carbon-rich residue, which then undergoes graphitization to form sp^2-hybridized graphene sheets [12]. The resulting graphene's quality and properties, such as electrical conductivity, surface area, and structural integrity, are influenced by laser power, speed, and points-per-inch (PPI) [8]. Improper settings can lead to incomplete graphitization, excessive ablation, or undesirable surface morphologies, negatively affecting electrochemical performance [13]. Conversely, optimal laser power can enhance graphitization, and a higher PPI can facilitate more controlled and uniform graphene formation. Therefore, fine-tuning these parameters is essential to optimize the electrode characteristics and enhance sensor performance.

This study focuses on optimizing the properties of LIG electrodes fabricated from polyimide by varying laser parameters (power, speed, and PPI) and evaluating the electrochemical performance of the electrodes. We investigated a series of electrodes fabricated under different parameters and identified the optimal set of parameters from a single laser pass that resulted in the best electrochemical performance in a standard redox solution (i.e., ferro/ferricyanide). Using these parameters, we fabricated and characterized additional electrodes with two and three laser passes. To enhance the durability of the often fragile LIG, we employed silver ink to print the electrodes' contact pads and connection wires.

The primary objective of this study is to enhance the electron transfer kinetics and overall performance of LIG electrodes for electrochemical sensing through systematic optimization. To demonstrate the enhanced performance of the optimized LIG electrodes, we electrodeposited nickel hydroxide ($Ni(OH)_2$) nanoparticles (NPs) onto the working electrode for non-enzymatic glucose detection as an application example. This achieved an ultrahigh sensitivity of 2577 $\mu A/cm^2$ mM glucose in 0.1 M NaOH with a fabrication cost of approximately $0.05 per strip. This study demonstrated the high performance of the optimized LIG electrodes, holding great promise for enhancing sensing performance in various applications.

II. METHODS

A. Fabrication of Electrode Pads, Leads, and Reference

Polyimide HN substrate (75 µm, DuPont) was cleaned with ethanol and ultrapure water, and Ag ink (Metalon NovaCentrix) was printed to create pads, connections, and the reference electrode. The pads were 3 mm x 5 mm, and the connection wires were 18.5 mm long and 1 mm wide. The printed Ag ink was cured at 80 °C for 1 hour.

United States National Science Foundation (Award#: 2138523)

B. Fabrication of Working and Counter Electrodes

Graphene was induced on the cleaned polyimide substrate using a 60 W CO_2 laser (Universal Laser Systems) with the optimized parameters: 4% power, 10% speed, and 1000 PPI, as listed in Table I. The working and counter electrodes were fabricated using these parameters with three laser passes. The working electrode has a diameter of 3 mm, while the counter electrode has an outer diameter of 6 mm and an inner diameter of 4 mm. The electrochemical characterization of the fabricated electrodes was performed using cyclic voltammetry (CV) in 5 mM $K_3Fe(CN)_6$ and 5 mM $K_4Fe(CN)_6$ using a CHI660A machine (CH Instruments).

TABLE I. RESISTANCE* WITH DIFFERENT LASER PARAMETERS

Power (%)	Speed (%)	R1 (Ω)	R2 (Ω)	R3 (Ω)	Average (Ω)
3	6	571	538	556	555
4	6	510	564	582	552
4	10	431	452	450	444
6	10	913	773	758	815
6	15	456	475	436	456
6	20	570	568	577	572
6	25	660	663	707	677

* Resistance was measured across a LIG wire of 1 mm × 18.5 mm.

C. Fabrication of Non-Enzymatic Glucose Sensor

$Ni(OH)_2$ NPs were electrodeposited onto the LIG electrode using a 10 mM nickel nitrate ($Ni(NO_3)_2$, Sigma-Aldrich) solution in UP water. The deposition was carried out by applying a constant potential of -1.5 V vs Ag pseudo reference electrode for 10 s. During this process, nitrate ions are electro-reduced to produce hydroxide ions (OH^-) locally, facilitating the formation of $Ni(OH)_2$ NPs on the LIG surface [14], as described in (1):

$$NO_3^- + 7H_2O + 8e^- \rightarrow NH_4^+ + 10OH^- \quad (1)$$

After deposition, the electrodes were gently rinsed with ultrapure water.

Following electrodeposition, the LIG-$Ni(OH)_2$ electrodes were further stabilized in 0.1 M NaOH solution by cycling potential from 0.1 to 0.8 V at a scan rate of 50 mV/s until the CV curves were stable (typically around 25 cycles). This stabilization step enhances the electrocatalytic properties of the $Ni(OH)_2$ NPs for glucose oxidation. The electrodes were then rinsed with UP water and dried overnight in a petri dish at room temperature.

For glucose sensing, the LIG-$Ni(OH)_2$ NPs electrodes were tested in a 0.1 M NaOH solution containing various glucose concentrations. 100 µL of the glucose solution was drop-casted onto the electrodes, and CV was conducted from 0.1 to 0.8 V at a scan rate of 50 mV/s. This procedure allowed us to evaluate the electrodes' catalytic performance for glucose oxidation.

III. RESULTS AND DISCUSSION

A. Characterization of LIG Electrodes

The electrical properties of the LIG electrodes were first assessed by measuring their resistance, as shown in Table I. The parameters that result in the lowest resistance (4% power, 10% speed, and 1000 PPI) were further investigated for multiple laser passes. As shown in Fig. 1(a), the average resistance decreased significantly with an increasing number of laser passes of up to 3 passes. The 1-pass LIG electrode showed the highest resistance (444 Ω). With 2 and 3 passes, the resistance dropped to 258 Ω and 233 Ω, respectively, indicating improved graphitization and enhanced electrical conductivity. The resistance showed minimal change (231 Ω for 4-pass electrodes) for further increase in the number of laser passes. This trend supports the hypothesis that multiple laser passes enhance the electrical properties of LIG by increasing graphene content and reducing defects.

The electrochemical performance of the LIG electrodes was evaluated using CV in a redox solution of 5 mM $K_3Fe(CN)_6$ and 5 mM $K_4Fe(CN)_6$. Screen-printed carbon electrodes (SPCE) were tested as the benchmark and showed the lowest redox peak current density of 0.99 mA/cm^2, as exhibited in Fig. 2(b). In contrast, all LIG electrodes exhibited higher peak current density than SPCE, reflecting an enlarged surface area. With the increasing number of laser passes, the redox peak current density increases, and the redox peak potential separation reduces, demonstrating enhanced surface area and improved electron transfer rate achieved by multiple laser passes. The 3-pass LIG exhibits the highest redox peak

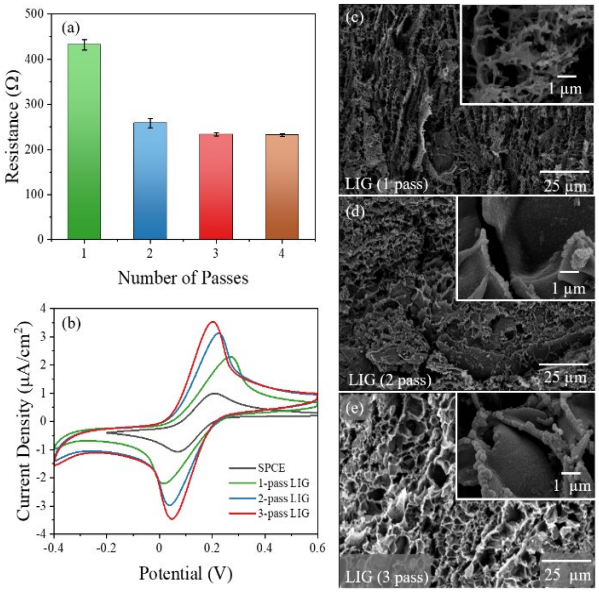

Fig. 1. Characterization of LIG electrodes fabricated with different numbers of laser passes. (a) Average resistance measurements for LIG electrodes with 1, 2, 3, and 4 laser passes. The resistance decreases with more laser passes, reflecting enhanced electrical conductivity. (b) Cyclic voltammogram (CV) of screen-printed carbon electrode (SPCE), LIG electrodes with 1, 2 and 3 passes, in a redox solution of 5 mM $K_3Fe(CN)_6$ and 5 mM $K_4Fe(CN)_6$ in UP water. The CV curves show increased peak currents and reduced redox peak separation with additional laser passes, indicating improved electrochemical performance. (c-e) FE-SEM images of LIG electrodes with (c) 1 pass, (d) 2 passes, and (e) 3 passes. The images reveal increased porosity and a more pronounced foamy structure with additional passes, suggesting enhanced graphitization and surface area. The insets show magnified views of the porous structures.

current density of 3.53 mA/cm^2, which is 3.5 times higher than that of the SPCE.

Field emission scanning electron microscopy (FE-SEM) images, as shown in Fig. 1(c)-(e), reveal significant differences in LIG electrodes with 1, 2, and 3 passes. The 1-pass surface appeared relatively smooth with small pores, indicating initial graphitization with incomplete conversion of polyimide. With the increasing number of laser passes, the electrodes showed increased porosity and a more pronounced foamy structure, suggesting enhanced graphitization for promoting electron transfer and improved surface area. These results align well with their electrochemical performance.

B. Glucose Sensing Performance of LIG-Ni(OH)$_2$

Electrodeposited Ni(OH)$_2$ NPs on LIG electrodes were first characterized by FESEM. As shown in Fig. 2(a), the LIG-Ni(OH)$_2$ electrodes maintained a highly porous structure with ultrafine nanoparticles decorated on the graphene surface.

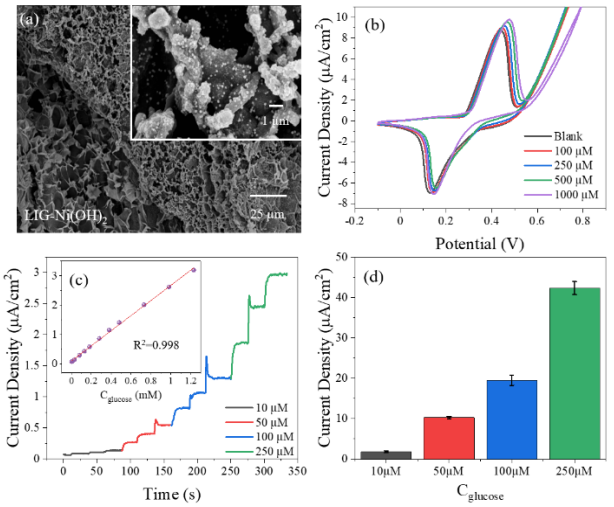

Fig. 2. Characterization and application of LIG electrodes modified with Ni(OH)$_2$ nanoparticles for non-enzymatic glucose sensing. (a) FESEM image of the LIG-Ni(OH)$_2$ electrode showing the porous structure and well-distributed Ni(OH)$_2$ nanoparticles. The inset provides a magnified view. (b) Cyclic voltammetry (CV) scans of the LIG-Ni(OH)$_2$ electrode in 0.1 M NaOH with varying glucose concentrations (100 μM, 250 μM, 500 μM, and 1000 μM). The increase in oxidation peak current with higher glucose concentrations indicates effective glucose detection. (c) Real-time amperometry data showing the current response to successive injections of low glucose concentrations (10 μM, 50 μM, 100 μM, and 250 μM). The inset depicts the linear relationship between the current response and glucose concentration. (d) Bar graph illustrating the change in current (Δ Current) for different glucose concentrations, demonstrating the electrode's high sensitivity and reliability for glucose detection.

The catalytic glucose oxidation behavior of the as-prepared LIG-Ni(OH)$_2$ electrodes was evaluated in 0.1 M NaOH with varying glucose concentrations (100 μM to 1000 μM). As presented in Fig. 2(b), an anodic peak and a cathodic peak can be observed at 0.44 and 0.13 V vs. Ag pseudo reference electrode, respectively, which can be ascribed to the reversible redox reaction between Ni(OH)$_2$ and NiOOH [15]. With increasing glucose concentration, the anodic peak current density increases, demonstrating the electrode's excellent electrocatalytic ability in glucose oxidation. The catalytic mechanism of the Ni(OH)$_2$ NPs toward glucose oxidation is shown in (2) and (3) [16]:

$$Ni(OH)_2 + OH^- \leftrightarrow NiOOH + H_2O + e^- \quad (2)$$

$$NiOOH + \text{glucose} \rightarrow Ni(OH)_2 + \text{glucolactone} \quad (3)$$

The high catalytic activity of the LIG-Ni(OH)$_2$ electrodes towards low concentration of glucose can be attributed to multiple factors: 1) the excellent catalytic property of the *in-situ* fabricated Ni(OH)$_2$ NPs, 2) the enhanced electron transfer rate through LIG optimization and the intimate contact between Ni(OH)$_2$ NPs and LIG through direct deposition without any binder or additives, 3) the high surface area provided by the interconnected porous structure of LIG.

Real-time amperometry detection of glucose using LIG-Ni(OH)$_2$ electrodes was carried out in 0.1 M NaOH at a constant applied potential of 0.4 V. Fig. 2(c) shows the stepwise current increases upon successive injections of glucose (3 additions of 10, 50, 100, and 250 μM glucose). The calibration curve presented in Fig. 2(c) inset reveals a linear relationship between current response and glucose concentration. The sensor demonstrated an exceptional sensitivity of 2577 μA/cm^2·mM glucose (based on the slope of the calibration curve) with a linear range from 0.01 mM to 1.23 mM. The limit of detection (LOD) was calculated to be 2.3 μM based on a signal-to-noise ratio of 3. The electrode's current responses toward various concentrations of glucose are presented in Fig. 2(d), indicating the electrode's reliability and consistency. The rapid and clear response to each glucose injection underscores the electrode's high sensitivity and potential for real-time glucose monitoring. Further validation of the sensors' selectivity, reproducibility, stability, and robustness will be carried out in the future.

IV. Conclusion And Future Work

This study demonstrated that optimizing parameters for fabricating LIG electrodes significantly enhances their electrochemical performance. By varying the power, speed, and PPI of the CO_2 laser, we identified optimal conditions for producing high-quality graphene electrodes. Our finding suggests that multiple laser passes facilitate graphitization for enhanced electron transfer and improved surface area. We further employed the optimized LIG electrodes and modified them with electrodeposited Ni(OH)$_2$ NPs for non-enzymatic glucose detection, demonstrating exceptional sensitivity and reliability. This study paves the way for developing high-performance, cost-effective, and scalable glucose sensors using LIG-Ni(OH)$_2$ electrodes, benefiting applications in medical diagnostics, personalized health monitoring, and industrial processes. Future work will focus on further enhancing sensor selectivity and integrating these sensors into portable, real-time monitoring systems.

Acknowledgment

We greatly appreciate the funding support from Michigan Technological University and the National Science Foundation (Award#: 2138523).

REFERENCES

[1] Hanrahan, G., Patil, D. G., & Wang, J. (2004). Electrochemical sensors for environmental monitoring: design, development and applications. Journal of environmental monitoring, 6(8), 657-664.

[2] Singh, K., Maurya, K. K., & Malviya, M. (2024). Review of electrochemical sensors and biosensors based on first-row transition metals, their oxides, and noble metals nanoparticles. Journal of Analysis and Testing, 8(2), 143-159.

[3] Maduraiveeran, G., Sasidharan, M., & Ganesan, V. (2018). Electrochemical sensor and biosensor platforms based on advanced nanomaterials for biological and biomedical applications. Biosensors and Bioelectronics, 103, 113-129.

[4] Zhu, Y., et al. (2010). Graphene and graphene oxide: synthesis, properties, and applications. Advanced materials, 22(35), 3906-3924.

[5] Santhiran, A., Iyngaran, P., Abiman, P., & Kuganathan, N. (2021). Graphene synthesis and its recent advances in applications—a review. C, 7(4), 76.

[6] Nam, J., Yang, J., Zhao, Y., & Kim, K. S. (2024). Chemical vapor deposition of graphene and its characterizations and applications. Current Applied Physics.

[7] Liu, B., & Ma, S. (2024). Precise synthesis of graphene by chemical vapor deposition. Nanoscale, 16(9), 4407-4433.

[8] Lin, J., et al. (2014). Laser-induced porous graphene films from commercial polymers. Nature Communications, 5(1), 1-8.

[9] Ye, R., James, D. K., & Tour, J. M. (2019). Laser-induced graphene: from discovery to translation. Advanced Materials, 31(1), 1803621.

[10] Ye, R., et al. (2015). In situ formation of metal oxide nanocrystals embedded in laser-induced graphene. ACS nano, 9(9), 9244-9251.

[11] Mamleyev, E. R., et al. (2019). Laser-induced hierarchical carbon patterns on polyimide substrates for flexible urea sensors. npj Flexible Electronics, 3(1), 1-11.

[12] Wang, F., et al. (2017). Formation of hierarchical porous graphene films with defects using a nanosecond laser on polyimide sheet. Applied Surface Science, 419, 893-900.

[13] Dong, Y., et al. (2016). Molecular dynamic simulation of layered graphene clusters formation from polyimides under extreme conditions. Carbon, 104, 47-55.

[14] Liu, Danqing, et al. "Electrodeposition of nickel hydroxide nanoparticles on carbon nanotube electrodes: correlation of particle crystallography with electrocatalytic properties." The Journal of Physical Chemistry C 120.29 (2016): 16059-16068.

[15] Kung, C.-W.; Cheng, Y.-H.; Ho, K.-C. Single Layer of Nickel Hydroxide Nanoparticles Covered on a Porous Ni Foam and Its Application for Highly Sensitive Non-Enzymatic Glucose Sensor. Sens Actuators B Chem 2014, 204, 159–166.

[16] Jafarian, M., Forouzandeh, F., Danaee, I., Gobal, F., & Mahjani, M. G. (2009). Electrocatalytic oxidation of glucose on Ni and NiCu alloy modified glassy carbon electrode. Journal of Solid State Electrochemistry, 13, 1171-1179.